NASA Technical Memorandum 105734
AIAA-92-3228

3D Rocket Combustor Acoustics Model

Richard J. Priem
Priem Consultants, Inc.
Cleveland, Ohio

and

Kevin J. Breisacher
Lewis Research Center
Cleveland, Ohio

NASA

3D ROCKET COMBUSTOR ACOUSTICS MODEL

Richard J. Priem
Priem Consultants Inc.
Cleveland, Ohio

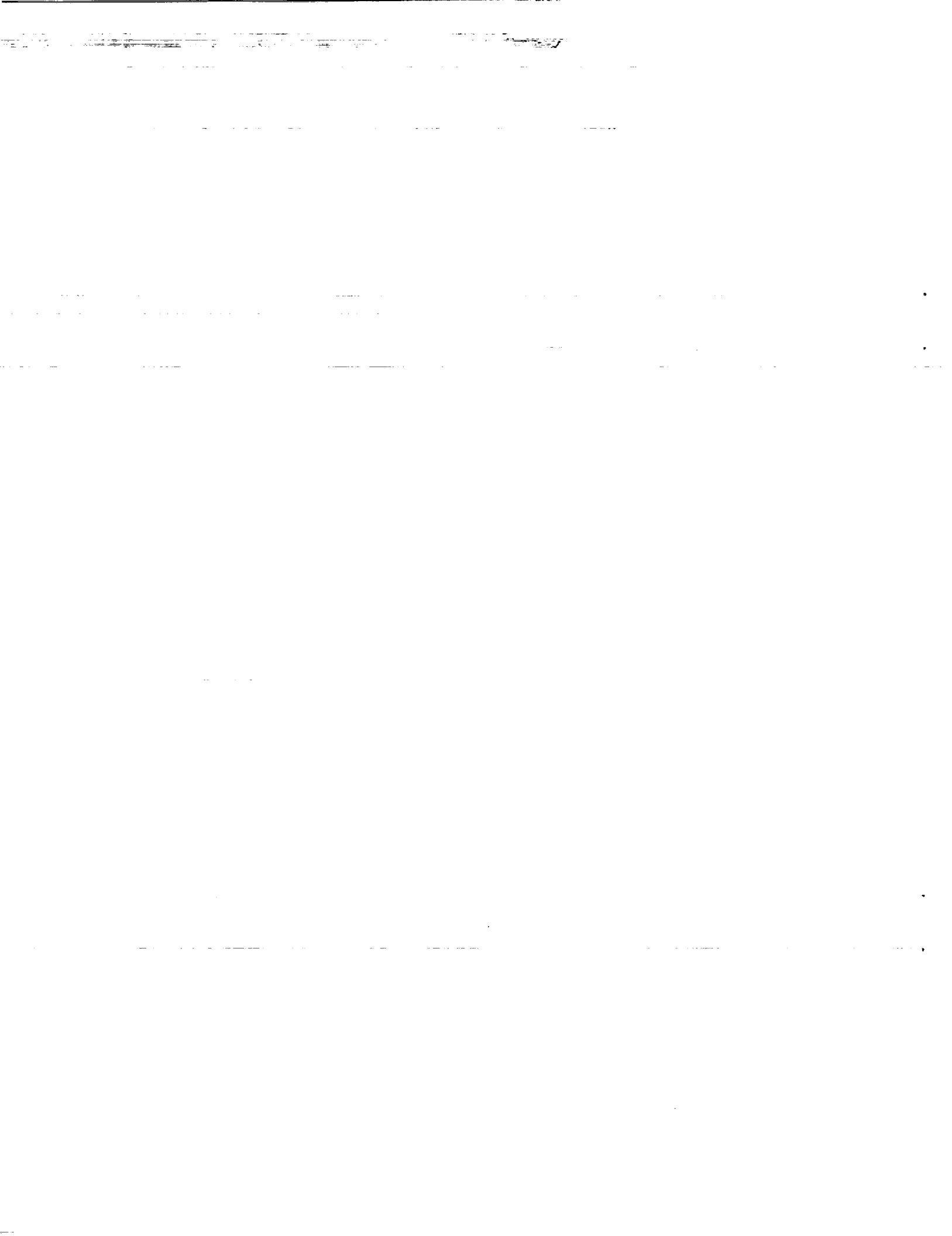Kevin J. Breisacher
NASA Lewis Research Center
Cleveland, Ohio

ABSTRACT

The theory and procedures for determining the characteristics of pressure oscillations in rocket engines with prescribed burning rate oscillations are presented. Analyses including radial and hub baffles and absorbers can be performed in one, two, or three dimensions. Pressure and velocity oscillations calculated using this procedure are presented for the SSME to show the influence of baffles and absorbers on the burning rate oscillations required to achieve neutral stability. Comparisons are made between the results obtained utilizing 1D, 2D, and 3D assumptions with regards to capturing the physical phenomena of interest and computational requirements.

INTRODUCTION

To understand and control combustion instability in liquid rocket engines requires detailed information about the combustion process and the characteristics of the oscillations in the engine. As we learn more about the combustion processes in rocket engines, it is apparent that combustion in a given region is very dependent on the local pressure and velocity histories. Therefore, trying to characterize instability by two numbers that represent the combustion process (i.e. n and tau or a combustion response number) is a gross simplification.

Studies [1-3] have provided equations relating the atomization process to the surrounding flow field. These equations can provide a description of the time dependent drop size and atomization rates across the face of the injector if the oscillating flow field is known. Coupling the atomization data with models for the vaporization process[4], a local burning rate can be determined that is dependent on local gas conditions. The HICCIP model described at the 1990 ETO conference[5] uses such a procedure. However, the previous model was restricted to using wave characteristics derived from a pseudo 3D theory. The model assumed uniform combustion response at all radial and tangential positions for a given axial position. Also, the wave model could not account for the presence of baffles and discrete absorbers. A fully 3D model was developed for HICCIP to predict the acoustic characteristics in realistic combustion chamber geometries. The basic theory and algorithms used in the model are described. Calculations for the SSME are presented to illustrate the main features of the model.

THEORY

The basic conservation equations used to define flow in a cylindrical chamber are:

CONSERVATION OF MASS:

$$\frac{\partial \rho}{\partial t} + \nabla \cdot (\rho V) = W$$

CONSERVATION OF MOMENTUM:

$$\frac{\partial (\rho V)}{\partial t} + \nabla \cdot \rho VV + g \nabla P = W V_{11q}$$

ADIABATIC IDEAL GAS:

$$\frac{P}{P_o} = \left(\frac{\rho}{\rho_o}\right)^{\gamma}$$

Where:

ρ	gas density, lb/in^3	
V	gas velocity vector, in/s	
P	pressure, lb/in^2	
t	time, s	
W	local burning rate, lb/in^3	
V_{liq}	velocity of burning liquid, in/s	
g	conversion constant, lbm in/lbf s^2 (386.4)	
∇	space derivative, in^{-1}	

It is assumed that viscous and gravitational forces are negligible. To simplify the analysis, it is further assumed that the radial and azimuthal steady or average flows are minimal and are therefore zero. This avoids requiring a 3D steady state or time average solution to determine radial and azimuthal flow and pressure profiles.

As in HICCIP, all the variables (P, ρ, V_z, V_r, V_θ, W) are expanded in a Fourier time series as given by:

$$F = F_o + F_1 e^{i\omega t} + F_2 e^{2i\omega t} + \ldots + F_n e^{ni\omega t} + \ldots$$

Where: F_o is the time averaged variable
F_n is a variable in all three dimensions

Consistent with the above assumptions:

ρ_o & P_o vary only in the axial direction
V_{ro} & $V_{\theta o}$ are zero (no radial or tangential average flow)
V_{zo} & W_o are variable in all three space dimensions.

All of the equations are nonlinear. In the remaining portion of this paper, only the terms through F_1 are used as these terms are not influenced by the F_2, and higher n terms (since low frequency cross products produce higher harmonic frequencies). After determining the F_1 values the equations could again be solved using the known F_o and F_1 values to find the F_2 values. This process could be continued to determine as many F_n values as required to "completely and rigorously" define the oscillations. Solutions for the F_1 values will define the complex frequency of the oscillations (both the observed frequency and the damping or growth rate).

Substituting the Fourier time series into the conservation equations and retaining only the terms containing "F_o and F_1" yields the following set of equations:

CONTINUITY:

$$i\omega \rho_1 + \frac{1}{r}\frac{\partial(r\rho_o V_{r_1})}{\partial r} + \frac{1}{r}\frac{\partial(\rho_o V_{\theta_1})}{\partial \theta} + \frac{\partial(\rho_o V_{z_1})}{\partial z} + \frac{\partial(\rho_1 V_{z_o})}{\partial z} = W_1 \qquad Eq.1$$

AXIAL MOMENTUM:

$$i\omega \rho_o V_{z_1} + i\omega \rho_1 V_{z_o} + 2\frac{\partial(\rho_o V_{z_o} V_{z_1})}{\partial z} + \frac{\partial(\rho_1 V_{z_o} V_{z_o})}{\partial z} + \frac{1}{r}\frac{\partial(r\rho_o V_{r_1} V_{z_o})}{\partial r} + \frac{1}{r}\frac{\partial(\rho_o V_{\theta_1} V_{z_o})}{\partial \theta} + \gamma\frac{P_o}{\rho_o}\frac{\partial \rho_1}{\partial z} = W_1 V_{liq} \qquad Eq.2$$

RADIAL MOMENTUM:

$$i\omega \rho_o V_{r_1} + \frac{\partial(\rho_o V_{z_o} V_{r_1})}{\partial z} + \gamma\frac{P_o}{\rho_o}\frac{\partial \rho_1}{\partial r} = 0 \qquad Eq.3$$

2

AZIMUTHAL MOMENTUM:

$$i\omega\rho_o V_{a_1} + \frac{\partial(\rho_o V_{z_o} V_{a_1})}{\partial z} + \gamma\frac{P_o}{r\rho_o}\frac{\partial P_1}{\partial\theta} = 0 \qquad\qquad Eq.4$$

ADIABATIC IDEAL GAS:

$$P_1 = \gamma\frac{P_o}{\rho_o}\rho_1 \qquad\qquad Eq.5$$

The boundary conditions for the combustor are:

Chamber Wall

$$V_{r_1} = \gamma\ RspWall\ P_1$$

where "RspWall" is zero for hard walls and is an input value for wall absorbers (RspWall is ratio of the radial velocity to local pressure).

Center of Chamber (r = 0)

All radial fluxes are zero as the area is zero.

Injector Face

$$V_{z_o} = 0 \qquad \frac{\partial\rho_1}{\partial z} = 0 \qquad \frac{\partial V_{a_1}}{\partial z} = 0 \qquad \frac{\partial V_{r_1}}{\partial z} = 0$$

$$V_{z_1} = \gamma\ RspInj\ p_1$$

where "RspInj" is zero for a solid injector face and is input for absorbers on the injector face.

End of Combustion Chamber

$$V_{z_1} = \gamma\ RspNoz\ \rho_1$$

Where "RspNoz" is the nozzle response obtained from another program, theory etc. as desired. (For this paper it is assumed to be zero - short distributed ideal nozzles)
and

$$\frac{\partial\rho_1}{\partial z}\quad,\quad \frac{\partial V_{a_1}}{\partial z}\quad,\quad \frac{\partial V_{r_1}}{\partial z}$$

3

are obtained from solutions of the wave equation with the chamber dimensions, exit gas velocity, and nozzle response specified.

Baffle surfaces

Radial Baffle $V_{ai} = 0$ Baffle is at an azimuthal momentum cell face.

Hub Baffle $V_{ri} = 0$ Baffle is at a radial momentum cell face.

Equations 1 - 4 result in a very sparse matrix when using finite difference equations as illustrated above. The number of terms in each equation are:

continuity   - 9 terms
axial momentum   - 13 terms
radial momentum   - 5 terms
azimuthal momentum - 5 terms.

The total number of equations and variables to be solved is determined by the number of cells used in each of the three dimensions as given by:

equations = variables = 4 * Ni * Nj * Nk

Where: Ni number of radial cells
         Nj number of azimuthal cells
         Nk number of axial cells.

As an example, for Ni=10, Nj=12, and Nk=20, which adequately defines an unbaffled chamber with the fundamental transverse mode we have 12,000 equations with complex variables. Each equation has an average of 8 unknowns. The "W" source term is specified for each cell and is determined using burning models as in HICCIP.

The resulting sparse matrix equations are solved using a conjugate gradient algorithm[5] modified for complex variables. Since the matrix is neither symmetric nor positive definite, a quadratic form of the error is minimized. This quadratic form effectively has the square of the condition number of the original matrix. As a result, it is necessary to use double precision on machines with 32 bit word sizes. The current algorithm does not incorporate preconditioning. Crude attempts to implement a "multigrid" solution procedure did not reduce computation time.

1D and 2D MODEL

It is also possible to model the oscillations as 1D or 2D phenomena. This is accomplished by assuming that the oscillations in the radial and/or azimuthal directions can be specified by an analytic wave equation solution in the desired direction as used in Ref 7. With this assumption, the momentum equation in that direction is not necessarily satisfied. The wave equation is:

$$\Phi = f(z) \, e^{i\omega t} e^{in\theta} J_r(mr)$$

and the variables are determined by:

$$p_1 = C \frac{\partial \Phi}{\partial t}$$

$$V_{z_1} = C \frac{\partial \Phi}{\partial z}$$

$$V_{r_1} = C \frac{1}{r} \frac{\partial \Phi}{\partial r}$$

4

$$V_{a_1} = C \frac{\partial \Phi}{\partial \theta}$$

For one cell, in the radial direction the radial derivatives in equations 1 to 5 are given as follows:

$$\frac{1}{r} \frac{\partial}{\partial r} (r \rho_o V_{r_1}) = \frac{\rho_o}{r} [\frac{\partial^2}{\partial r^2} (r J_n(mr)) / \frac{\partial}{\partial r} (J_n(mr))] V_{r_1}$$

$$\frac{1}{r} \frac{\partial}{\partial r} (r \rho_o V_{z_o} V_{r_1}) = \frac{\rho_o V_{z_o}}{r} [\frac{\partial^2}{\partial r^2} (r J_n(mr) / \frac{\partial}{\partial r} J_n(mr)] V_{r_1}$$

$$\gamma \frac{P_o}{\rho_o} \frac{\partial \rho_1}{\partial r} = \frac{\gamma P_o}{\rho_o} [\frac{\partial}{\partial r} (r J_n(mr)) / J_n(mr)] \rho_1$$

where the Bessel derivative terms are determined from Bessel function tables (at a radius equal to half the chamber radius) for different Bessel Function indices "m and n" which describe the mode in the radial direction and the tangential mode (n). The calculations then correspond to a very thin annular ring at half the distance to the chamber wall.

Similarly for only one cell in the azimuthal direction the azimuthal derivative in equations 1 to 5 are given as follows:

$$\frac{1}{r} \frac{\partial \rho_o V_{a_1}}{\partial \theta} = i \frac{n}{r} V_{a_1}$$

$$\frac{1}{r} \frac{\partial (\rho_o V_{z_o} V_{a_1})}{\partial \theta} = \frac{\rho_o V_{z_o}}{r} i n V_{a_1}$$

$$\frac{1}{r} \frac{\partial (\rho_o \rho_1)}{\partial \theta} = \frac{\gamma \rho_o}{r} i n \rho_1$$

where n specifies the number of modes in the azimuthal direction. The calculations then correspond to a very thin "pie" section cut out of the chamber.

RESULTS

Calculations were made for the SSME and conditions similar to those used by Wieber[7] in his cold flow tests of baffled chambers.

SSME SIMULATION

For the SSME calculations, a time averaged combustion profile was assumed similar to that obtained with a vaporization limited model (50% of combustion completed 2.3 inches from the injector, 90% completed in 7.5 inches, and 99% complete combustion within the chamber). The time averaged combustion profile remained constant (the average combustion rate at all positions is independent of the oscillations). This average profile is not a realistic assumption as the oscillations do influence the time averaged burning rate. The influence of the gas oscillations will be demonstrated later when the 3D wave dynamics solution is combined with the combustion models in HICCIP.

Burning rate oscillations were obtained by using a combustion response that was assumed not to vary spatially. This also is a simplistic assumption. However, the assumption of a constant combustion response permits us to demonstrate the wave dynamics model and indicates the influence of chamber geometry on stability margin for the SSME.

The definition for combustion response is:

$$\text{CombRsp} = \frac{W_i / W_o}{P_i / P_o}$$

where:
- W_i is the perturbation in burning rate, $lb/(s\ in^3)$
- W_o is the local average burning rate, $lb/(s\ in^3)$
- P_i is the perturbation in pressure, psi
- P_o is the local average pressure, psi

The combustion response is a vector in the complex plane. The real portion of the combustion response is the magnitude of the nondimensional burning rate oscillation that is in phase with the pressure. The imaginary portion of the combustion response indicates the phasing of combustion relative to pressure. A positive imaginary response indicates that the combustion is leading the time dependent pressure, a negative indicates combustion is lagging.

The combustion response needed to drive various oscillations in the SSME were determined iteratively. For a given frequency, a combustion response was assumed, and a burning rate oscillation was determined using an acoustic wave solution. The assumed burning rate oscillation was used as an intial guess to determine oscillating pressure and velocity profiles in the combustor. With the calculated pressure profile and assumed burning rate oscillations, a mass averaged combustion response was calculated. Using the mass averaged combustion response and calculated pressure profiles, a new burning rate oscillation was calculated. The process was then repeated until the change in the burning rate was less than 0.003 between successive calculations.

SSME CONFIGURATION

Chamber Diameter	17.74	in.
Cylindrical Length	15.079	in.
Hub Baffle Length	2.0	in.
Hub Baffle Diameter	8.87	in.
Radial Baffles	5	blades
Radial Baffle Length	2.0	in.
Chamber Pressure	2844	psia
Oxidizer Flow	834.0	lbs/s
Fuel Flow	225.3	lbs/s
Absorber Wall Gap	0.36	in.
Absorber Tuned Freq	3T	Mode
Speed of Sound	5183	ft/s

Figure 1

Using this configuration a combustion response for any frequency can be determined. Calculations were made (with a grid size of 4 radial, 10 azimuthal, and 8 axial cells) for the 1T mode and the results are shown in Fig. 1. The complex combustion response is plotted as a function of frequency between 1800 and 2000 Hz. Three curves are shown corresponding to damping rates of neutral (0.0) and + or - 628 s⁻¹. As the frequency is increased, the combustion response changes from combustion lagging pressure to combustion leading pressure and is in phase (1.24 real and zero imaginary) at 1893 Hz with neutral stability. Normally, this is considered the "natural frequency" of the 1T mode for this engine. However, if the combustion response does not have this value the engine can operate at another frequency as shown in Fig. 1. Larger real combustion responses make the engine unstable, lower values result in a more stable engine. Negative imaginary combustion response lowers the tuned frequency and positive imaginary combustion response increases the tuned frequency. Similar plots can be obtained for all the
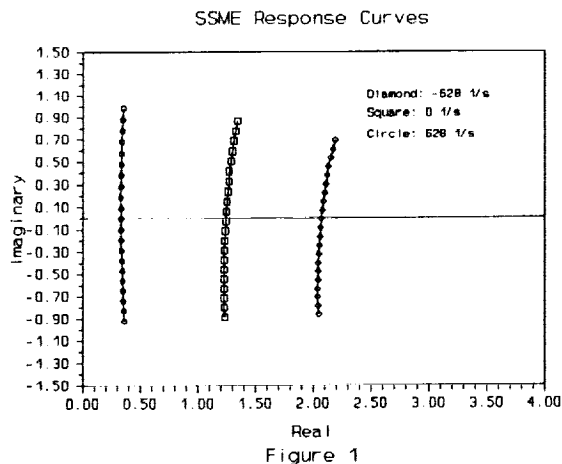
possible modes in the chamber. The mode type is determined in these calculations by the initial assumption for the pressure profile or burning rate oscillations in the chamber.

To illustrate the influence of design parameters on stability and stability modes, calculations were made to determine the frequency and combustion response for neutral stability at the natural frequency, i.e. where the combustion response has no imaginary value and the oscillations have a zero growth or decay rate. The results of these calculations for different "SSME configurations" and modes are presented in TABLE I.

TABLE I

NEUTRAL STABILITY CONDITIONS FOR SSME

Mode	Frequency	Response	
UNBAFFLED AND NO ABSORBER			Grid of 8*1*16
1 L	1966	1.69	
1 T	2057	1.69	
2 T	3407	1.65	
3 T	4686	1.64	
UNBAFFLED AND ORIGINAL SSME ABSORBER			Grid of 8*1*16
1 L	1955	1.73	
1 T	2045	1.63	
2 T	3366	1.50	
3 T	4680	2.63	
UNBAFFLED AND TUNED 1T ABSORBER			Grid of 8*1*16
1 L	1966	1.94	
1 T	2052	1.90	
2 T	3403	2.51	
3 T	4680	2.63	
BAFFLED AND ORIGINAL SSME ABSORBER			Grid of 8*20*16
1 L	1955	1.73	
1 T	1957	1.65	
2 T	3023	1.08	
3 T	4305	2.26	

Table I illustrates how the acoustic absorber improves stability in the SSME. The original absorber design is tuned to the 3T mode and increases the combustion response of the 3T mode necessary for neutral stability from 1.64 to 2.63. This is equivalent to going from neutral stability to a damping rate of -628 s^{-1} in Fig. 1. A damping rate of this magnitude would decrease the amplitude of a 100% peak-to-peak wave to the one tenth of initial amplitude in 3.6 milliseconds. The damping rate as required by Ref. 10 is 18 milliseconds. Therefore, the SSME absorber design provides a damping five times that required for the 3T mode.

The original absorber design provides a very small change in chamber frequency and response for the 1T and 1L mode because the absorber is tuned to a much higher frequency. The 2T mode is actually made more unstable by the absorber because it reduces the tuned frequency and decreases the required response. Retuning the SSME absorber to the 1T and 1L modes by decreasing the opening in the chamber from 0.36 in. to 0.12 in. and increasing the aperture length from 0.5 in. to 1.0 in. will produce a large increase in stability, more than enough to meet the damping requirements of Ref. 10. The increase in stability at the 1T and 1L frequencies is small because the absorber opening has been reduced from 0.36 in. to 0.125 in. to obtain tuning at these frequencies.

The addition of the five bladed hub baffle to the SSME changes the tuned frequencies and slightly decreases the response required for neutral stability. The frequency change is 105 Hz for the 1T mode and 380 Hz for the 2T mode. The reduction in response is also greater for the 2T mode. These calculations show that oscillations can occur with baffled chambers. Oscillations with either standing or spinning wave characteristics could be achieved. In the presence of the baffle, the wave is distorted within and near the baffles compartments, but an acoustic like wave does exist. The decrease in response occurs because of the wave distortion produced by the baffles when coupled with the steady flow profile within the chamber. The baffles reduce the loss associated with the steady flow convecting the oscillations out of the chamber. Thus the major influence of the baffles on stability margin must be to change the pressure and velocities in the combustion zone which determine how combustion processes can produce burning rate oscillations. It will be possible to gauge this effect when the wave dynamics solution is incorporated in HICCIP.

COMPARISON WITH WIEBER COLD FLOW TESTS

To test the capability of the present approach to calculate observed acoustic phenomena, calculations were performed for comparisons with the results published by Wieber[7]. Wieber made measurements of resonant

frequencies in baffled and unbaffled chambers driven by an acoustic speaker. The experimental and calculated results for a cylindrical chamber 6 inches in diameter and 6 inches in length are presented in Table II.

TABLE II
COMPARISON WITH WIEBER DATA

NO BAFFLES   Speed of Sound = 1159 ft/sec   Grid 8*1*16

Mode	THEORY	EXPERIMENTAL Frequencies (Hz)	CALCULATED	% Dif
1 L	1159	1241	1167	-5.5
1 T	1358	1367	1358	+0.1
2 T	2253	2257	2263	+1.0
3 T	3099	3095	3100	+0.9

FOUR 3 INCH BAFFLES   Grid 6*16*12

Mode			
1 Tst		786	
1 T	858		
	885		
2 Tst1/2L		907	
2 T	2300	2224	-3.4
4 Tst1/2L		2407	
3 T	3080		
3 Tst 1L		2951	-4.3

These results indicate agreement within the experimental accuracy. No measurement was reported of the speed of sound within the chamber during the tests. Also, the experimental resonant frequency was determined by adjusting the frequency to obtain maximum pressure amplitudes. If the acoustic drivers have a phasing between movement and pressure, then the driving does not compare to our neutral stability criteria (driving in phase with pressure). The agreement between calculated and experimental frequencies with unbaffled chambers is very good.

Natural frequencies with baffled chambers were much more difficult to measure experimentally and find using the computer. The long baffles lowered the natural frequencies and significantly distorted the waves. According to Wieber[7] ,"predicted pressure nodes could not be detected ... the resulting acoustic fields appeared to be combinations of spinning and standing modes with complex small-scale spatial phase relation". The calculated modes were difficult to generate as a good guess of the the initial profile that would result in the desired distorted wave was necessary. Distinct neutral modes were found, all of which were standing on the baffles. All of the wave shapes were distorted and did have complex small-scale spatial phase relations. Two frequencies were identified by Wieber as 1T modes, which depended on whether he drove the waves on a baffle or in a baffle pocket. Calculations showed two solutions near these reported frequencies, a 1T at 786 Hz and a 2 T 1/2 L (amplitude of the oscillation is very small at the nozzle) at 907 Hz. These waves were very complex and did not have pressure antinodes. Mode number was identified by determining the number of times that the real and imaginary pressure perturbations go through zero in a given direction in the unbaffled section of the cylinder. It would be very easy to interpret the 2T 1/2 L mode as being a 1T mode by probing the wave with a single microphone as used by Wieber.

Wieber also measured damping rates of the oscillations after the driver was turned off. While these were noticeable (0.12 decay per cycle or 86 /sec) with the baffled chamber, this represents very little loss in a real combustion chamber. The burning rate oscillation required for this damping with no flow in the chamber is equivalent to less than a 0.01 combustion response with the flow field in the SSME.

Additional comparisons were made with the cold flow and hot fire data collected during the Gemini Stability Improvement Program (GEMSIP).[9] Calculations were made for both cold flow and hot fire (finite Mach number) conditions for a seven bladed baffle geometry. The baffle length was changed to assess the impact on the frequency of the 1T mode. The calculated results were normalized to the zero baffle length data to account for uncertainties in experimental acoustic velocities and flowrates. The code captures the frequency depression trends well (Fig. 2). The "Strahle" of banana baffle geometry was simulated as a hub baffle with two radial blades 180 degrees apart. As expected, the frequency depression effects were suppressed.

The calculated results were somewhat dependent on the grid size used in the calculations as shown in TABLE III.

1 - Long 7H
2 - Long 7H/Lid
3 - Long 7
4 - Cant 5
5 - Cant 5/Lid
6 - Titan 6
7 - Titan 6 Full Scale
8 - Wing 7B
9 - Wing 7A
10 - Flush 7

11 - Wing 7
12 - Unbaffled Half & Full Scale
13 - "Strahle"
14 - Unbaffled (Hot Fire) Normalized
     Unbaffled (Full Scale) Normalized
     Unbaffled
15 - Titan 6H (Hot) Normalized
16 - Long 7, Canted 5 (Hot) Normalized

f = Frequence of Mode (cps)
d = Diameter of Chamber (ft)
c = Speed of Sound (cold = 1130 ft/sec)(hot = 3800 ft/sec)
h = Height of baffle = area/radial length

δ = Decay rate $\frac{db}{sec}$

Hot Fire Calculated

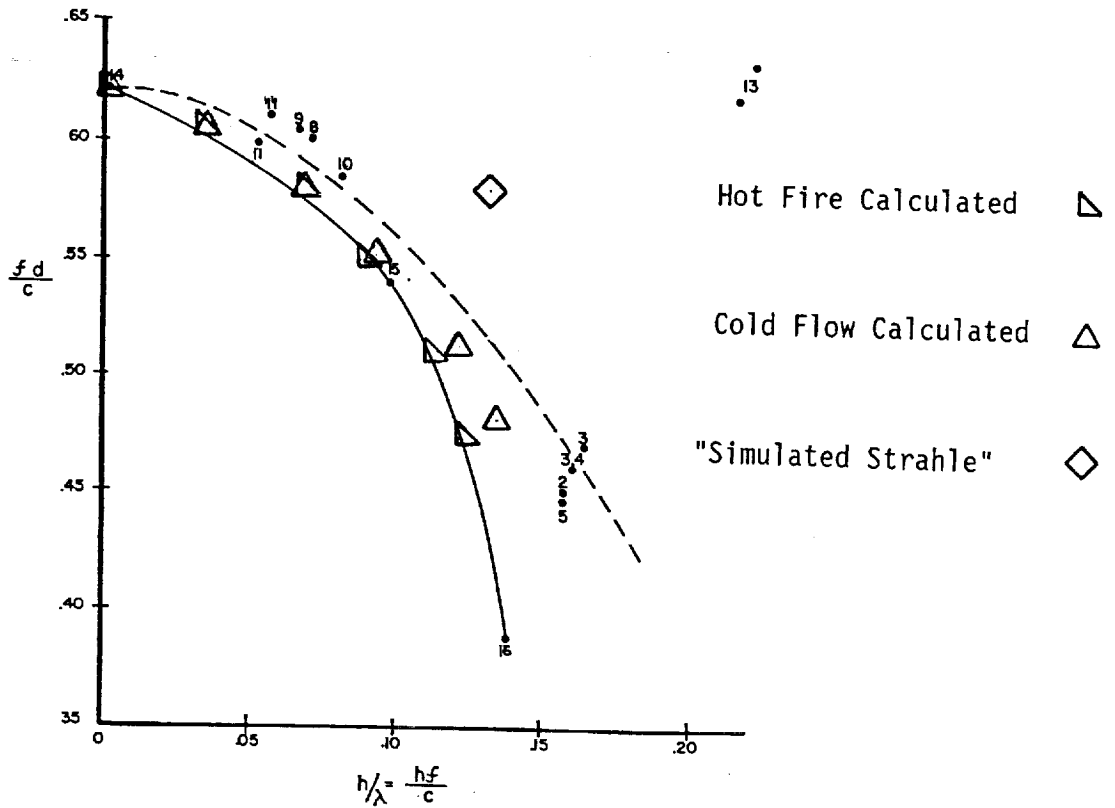Cold Flow Calculated

"Simulated Strahle"

Figure 2. Effect of Baffle Height on 1T Frequency Depression

TABLE III

INFLUENCE OF GRID SIZE ON SSME CALCULATIONS - 1 T MODE

Grid Size	Freq	Response
UNBAFFLED CHAMBER - NO ABSORBER	1 T MODE	
1*1*16	2052	1.66
4*1*8	2057	1.69
8*1*16	2057	1.69
16*1*32	2057	1.70
8*20*8	2057	1.68

Very good agreement is obtained for unbaffled chambers with different grid sizes. With these conditions the oscillations are relatively smooth functions and excellent agreement is obtained with a very coarse grid. Adding baffles to the chamber distorts the wave and changes the tuning frequency. This wave shape is difficult to capture in great detail with a coarse pattern.

COMPUTATION TIMES

The model has been used to determine wave characteristics with different number of cells and boundary conditions using different computers. An example of the CPU times for calculations to obtain a solution for a specified oscillating burning rate in each cell and a time averaged flow are:

TABLE IV

COMPUTATION TIME FOR SINGLE SOLUTION - 1 T MODE

Cell Size			Model	COMPUTER TYPE
				TIME
Ni	Nj	Nk		486 (33MHz)
1	1	16	Cylinder	0.05 Min
4	1	8	"	0.07 "
8	1	16	"	2.30 "
16	1	32	"	18.19 "
4	10	8	Baffled	0.03 Hrs
8	20	16	"	1.62 Hrs
8	20	32	"	8.03 Hrs

After a computation to determine the flow oscillations with a specified oscillating burning rate, the burning rate is not necessarily consistent with oscillations one would expect from burning submodels. Therefore, the process has to be repeated several times (3 to 10 depending on the initial guess) before the burning rate agrees with the oscillations. Typical computational times for completing this type of calculation (equivalent to determining the complex frequency with a given combustion model) is:

COMPUTATION TIME FOR RESPONSE (FREQUENCY) SOLUTION - 1T MODE

Cell Size			Model	COMPUTER TYPE		
Ni	Nj	Nk		486 (33MHz)	VAX (8600)	Cray (YMP-8)
1	1	16	Cylinder	0.15 Min		
4	1	8	"	0.22 Min		
8	1	16	"	4.7 Min		
16	1	32	"	39.4 Min		
4	10	8	Baffled	6.6 Min	1.3 Min	
8	20	16	"	3.19 Hrs	1.55 Hrs	4.04 Min
8	20	32	"	13.7 Hrs	8.27 Hrs	8.34 Min

Computation time is dependent on the initial guess for the burning rate oscillations. If a very poor guess is made, many more iterations are required before the burning rate oscillations agree with the calculated pressure profile and constant combustion response assumption. If a frequency scan is used and the solution from the last frequency is used as the next assumption, the compution times shown above can be decreased by as much as a factor of 4. Similarly, higher order modes and/or frequencies require significantly less computation time (as much as 1/3 for the 3T mode). Compution times are smaller when the original guess for the pressure and velocity perturbations are zero. This allows the perturbations to grow to the correct value which is faster than correcting a large number that are slightly in error. However, a good initial guess for the burning rate oscillation is still important.

SUMMARY

The theory and algorithms used to calculate the wave dynamics in combustion chambers containing combinations of hub baffles, bladed baffles, and discrete absorbers has been outlined. Calculations using this approach have indicated the following:

1. Computation times to calculate a solution at a given frequency appear reasonable.

2. Oscillations can be present in baffled chambers with either spinning or standing characteristics.

3. Calculated natural frequencies in cold flow chambers agree with the experimental data and provide insight into the type of oscillations that may be present.

4. Baffles in the SSME change the natural frequency of oscillations and reduce the combustion response required to sustain oscillations. The SSME acoustic absorber changes the chamber tuning frequency and decreases stability for the 1L, 1T and 2T modes. The absorber also improves stability for the 3T mode more than required for dynamic stability.

REFERENCES

1. Wu, P. K., Ruff, G.A., and Faeth, G.M., Primary Breakup in Liquid/Gas Mixing Layers, AIAA Paper 91-0285 29th Aerospace Sciences Mtg., Jan. 7-10, 1991

2. Wu, P. K, Tseng, L.-K., and Faeth, G.M., Primary Breakup in Gas/Liquid Mixing Layers for Turbulent Liquids, AIAA Paper 92-0462 30th Aerospace Sciences Mtg. Jan. 6-9, 1992

3. Giridharan, M. G., A Computer Model for Liquid Jet Atomization in Rocket Thrust Chambers, NAS8-38425, Dec. 1991

4. Priem, R.J. Calculating Vaporization Rates in Liquid Rocket Engines Above Critical Pressure-Temperature Conditions., 27th JANNAF Combustion Subcommittee Meeting, Nov. 1991.

5. Priem, R.J. and Breisacher, K.J., High Frequency Injection Coupled Combustion Instability Program (HICCIP) Status and Plans, 1990 Conference on Advanced Earth-To-Orbit Propulsion Technology, Marshall Space Flight Center.

6. Numerical Recipes, Cambridge University Press, 1986.

7. Wieber, P.R., Acoustic Decay Coefficients of Simulated Rocket Combustors. NASA TN D-3425, May 1966.

8. Maslen, S.H. and Moore, F.K.,On Strong Transverse Waves Without Shocks in a Circular Cylinder, J. Aeron. Sci. 23, 583 (1956)

9. Gemini Stability Improvement Program Final Report, Vol. 5, Aerojet General, August, 1965.

10. Anom, Guidelines for COMBUSTION STABILITY SPECIFICATIONS AND VERIFICATION PROCEDURES for Liquid Propellant Rocket Engines. CPIA Publication 247 October 1973.

REPORT DOCUMENTATION PAGE

Public reporting burden for this collection of information is estimated to average 1 hour per response, including the time for reviewing instructions, searching existing data sources, gathering and maintaining the data needed, and completing and reviewing the collection of information. Send comments regarding this burden estimate or any other aspect of this collection of information, including suggestions for reducing this burden, to Washington Headquarters Services, Directorate for information Operations and Reports, 1215 Jefferson Davis Highway, Suite 1204, Arlington, VA 22202-4302, and to the Office of Management and Budget, Paperwork Reduction Project (0704-0188), Washington, DC 20503.

1. AGENCY USE ONLY (Leave blank)	2. REPORT DATE	3. REPORT TYPE AND DATES COVERED
	July 1992	Technical Memorandum

4. TITLE AND SUBTITLE

3D Rocket Combustor Acoustics Model

5. FUNDING NUMBERS

WU–590–21–21

6. AUTHOR(S)

Richard J. Priem and Kevin J. Breisacher

7. PERFORMING ORGANIZATION NAME(S) AND ADDRESS(ES)

National Aeronautics and Space Administration
Lewis Research Center
Cleveland, Ohio 44135–3191

8. PERFORMING ORGANIZATION REPORT NUMBER

E–7137

9. SPONSORING/MONITORING AGENCY NAMES(S) AND ADDRESS(ES)

National Aeronautics and Space Administration
Washington, D.C. 20546–0001

10. SPONSORING/MONITORING AGENCY REPORT NUMBER

NASA TM–105734
AIAA–92–3228

12a. DISTRIBUTION/AVAILABILITY STATEMENT

Unclassified - Unlimited
Subject Category 20

12b. DISTRIBUTION CODE

13. ABSTRACT (Maximum 200 words)

The theory and procedures for determining the characteristics of pressure oscillations in rocket engines with pre-scribed burning rate oscillations are presented. Analyses including radial and hub baffles and absorbers can be performed in one, two, or three dimensions. Pressure and velocity oscillations calculated using this procedure are presented for the SSME to show the influence of baffles and absorbers on the burning rate oscillations required to achieve neutral stability. Comparisons are made between the results obtained utilizing 1D, 2D, and 3D assumptions with regards to capturing the physical phenomena of interest and computational requirements.

14. SUBJECT TERMS

Combustion instability; Acoustics; Computer code

15. NUMBER OF PAGES

12

16. PRICE CODE

A03

17. SECURITY CLASSIFICATION OF REPORT	18. SECURITY CLASSIFICATION OF THIS PAGE	19. SECURITY CLASSIFICATION OF ABSTRACT	20. LIMITATION OF ABSTRACT
Unclassified	Unclassified	Unclassified	